Catalysis Today 139 (2008) 43–48

Contents lists available at ScienceDirect

Catalysis Today

journal homepage: www.elsevier.com/locate/cattod

The simultaneous catalytic removal of VOCs and O_3 in a post-plasma

Haibao Huang, Daiqi Ye *, Xiujuan Guan

College of Environmental Science and Engineering, South China University of Technology, Guangzhou 510006, PR China

ARTICLE INFO

Article history:
Available online 25 September 2008

Keywords:
Non-thermal plasma
Post-plasma
Toluene
Catalysis
Catalytic ozonation

ABSTRACT

The use of non-thermal plasma (NTP) technology for volatile organic compounds (VOCs) control has been limited because of its drawbacks. Although the combination of catalysis in plasma can avoid some of the limitations, there are still disadvantages such as the O_3 byproduct. In this study, catalysts were combined in the post-plasma. It is found that not only O_3 is efficiently eliminated, but also the removal of toluene is greatly enhanced due to O_3 decomposition. The effect of catalysts, humidity and the initial O_3 concentration on simultaneous catalytic removal of toluene and O_3 was studied. Results show that the performance of catalysts for toluene conversion is closely related to that for O_3 decomposition. The increase of O_3 concentration benefits toluene conversion, whereas water has a negative effect on the toluene conversion. Catalytic ozonation is mainly responsible for the toluene decomposition in the post-plasma.

1. Introduction

The emission of volatile organic compounds (VOCs) by various industrial processes and human activities is an important source of air pollution. VOCs do great harm to the environment and human health because of their toxicity, destruction of the ozone layer and through photochemical smog. Non-thermal plasma (NTP) technology has been widely investigated for the removal of dilute VOCs from many industries due to its unique properties, such as quick response at ambient temperature, high-energy electrons with short residence times, and system compactness [1,2]. However, NTP alone has many disadvantages, such as low energy efficiency, low CO_2 selectivity and undesired byproduct formation [3–6].

Many studies have been carried out to overcome the limitations of NTP through the combination of catalysis in plasma [1,7–10]. Although this can avoid some of the limitations of NTP, there are still drawbacks, such as incomplete elimination of O_3 and unsatisfactory efficiency of oxidation of VOCs [1,5]. O_3 is usually regarded as a hazardous byproduct in pollution control via NTP and must be removed before emission, as it is a strong oxidant. An option to overcome O_3 pollution is a combination of catalysts in the post-plasma. The post-plasma is the area downstream of the plasma. O_3 can be catalytically decomposed into active oxygen, and active oxygen can efficiently oxidize residual VOCs.

In this study, catalysts were combined in the post-plasma. Toluene was used as a representative VOC. The goals are to enhance toluene oxidation by utilizing O_3 in the post-plasma, to study factors such as choice of catalysts, humidity and O_3 concentration, and to investigate the plausible reaction pathway.

2. Experimental

2.1. Experimental set up

The experimental setup was described in a previous paper [11]. Two gas-feeding methods were tested (Fig. 1). In method (a), toluene was introduced before the plasma. In method (b), toluene was directly introduced into the post-plasma, in which the decomposition of toluene by NTP is excluded and the study on the effect of toluene and O_3 removal in the post-plasma is simplified. The gas was normally fed by method (b). The air flow rate, the initial toluene concentration and humidity at the inlet of the post-plasma reactor were 0.2 L/min, 100 ppmv, and 0.5 wt.%, respectively.

2.2. Reactor

A wire-plate dielectric barrier discharge (DBD) reactor was used in the experiment. The simplified structure of DBD reactor is shown in Fig. 2.

The epoxy resin board was used as dielectric barriers (the dielectric constant is $\varepsilon = 3.6$). The length, width and thickness of the board were 240, 50 and 0.8 mm, respectively. The high voltage electrode (HV) was made of copper wire, 0.8 mm in diameter. The wire-to-wire distance was 10 mm. A piece of nickel foam (150 mm × 25 mm × 2 mm) loaded with catalysts was stuck on

* Corresponding author. Tel.: +86 20 39380516; fax: +86 20 39380518.
E-mail address: cedqye@scut.edu.cn (D. Ye).

0920-5861/$ – see front matter © 2008 Elsevier B.V. All rights reserved.
doi:10.1016/j.cattod.2008.08.029

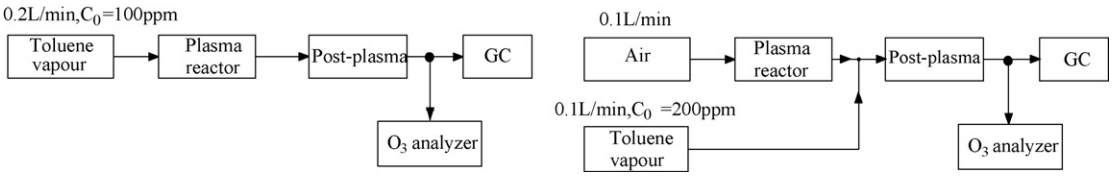

Fig. 1. Gas-feeding methods: (a) before plasma and (b) after plasma.

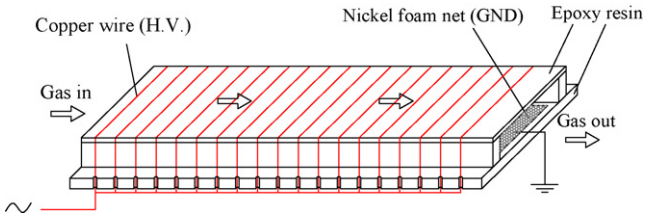

Fig. 2. Simplified structure of DBD reactor.

the epoxy resin board and acted as the grounded electrode (GND). The gap spacing of discharge was 10 mm.

The post-plasma reactor was cylindrical and connected to the DBD reactor in series. This reactor was made of quartz glass, with an outer diameter of 30 mm, an effective length of 150 mm and a thickness of 1 mm.

2.3. Catalysts

The catalysts were loaded on the porous nickel foam. CuO, Co_3O_4, Mn_2O_3, and Fe_2O_3 catalysts were prepared by impregnation with a calcining temperature of 600 °C. TiO_2 catalyst was prepared by impregnation using commercial P-25 (Degussa). The BET surface area was calculated from the nitrogen adsorption isotherms at 77 K with a surface area analyzer system (Micromeritics, ASAP2010).

Gas samples from the effluent were analyzed on-line by a gas chromatograph (Kechuang, GC-900A) and O_3 analyzer (Lida, DCS-1), respectively. The experiment was carried out at room temperature and atmospheric pressure.

3. Results and discussion

3.1. Comparison of Mn_2O_3 in the post-plasma and in plasma

Mn_2O_3 was placed in plasma or in the post-plasma via gas-feeding method (a), respectively. The toluene conversion and O_3 concentration at the outlet as a function of energy density were compared (Fig. 3). It was found that the removal efficiency of toluene in the system with Mn_2O_3 in the post-plasma was improved by nearly 40% compared with the plasma-only system, and by 5% compared with the system with Mn_2O_3 in the plasma, respectively. The concentration of O_3 at the outlet in the system with Mn_2O_3 in the post-plasma was decreased by nearly 90% and 60%, respectively. The combination of Mn_2O_3 in the post-plasma not only improved the conversion of toluene but also considerably enhanced O_3 decomposition. It can also be seen in Fig. 3 that the conversion of toluene is in negatively correlated with the O_3 concentration at the outlet, i.e., positively correlated with O_3 conversion.

O_3 was transported to the catalyst and decomposed into active oxygen on its surface. Active oxygen formed from O_3 catalytic decomposition is a strong oxidant, and it can effectively oxidize toluene. When Mn_2O_3 was placed in the post-plasma, toluene was decomposed not only by high-energy electrons in the plasma but

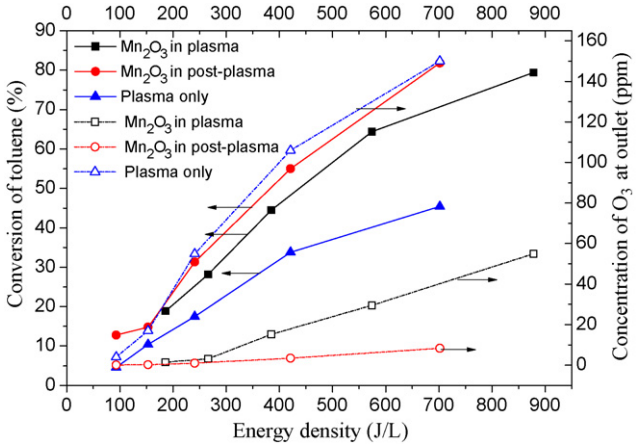

Fig. 3. Toluene conversion and O_3 concentration at the outlet as a function of energy density in plasma-only system, systems with Mn_2O_3 in plasma or in the post-plasma, respectively.

also by catalytic ozonation in the post-plasma. As a result, the removal of toluene in the system with Mn_2O_3 in the post-plasma is higher than in the system with Mn_2O_3 in the plasma. In the case of the system with Mn_2O_3 in the plasma, O_3 can be continuously formed after catalytic decomposition by Mn_2O_3. However, O_3 is not regenerated in the post-plasma. Therefore, the combination of Mn_2O_3 in the post-plasma can more effectively decrease the O_3 concentration at the outlet.

Guo et al. [12] reported that catalysts combined in the plasma could enhance the CO_2 selectivity and carbon balance compared with a plasma-only system. Fig. 4 shows the CO_2 selectivity and carbon balance in plasma and in the post-plasma with the alternative gas-feeding methods. CO_2 selectivity increased and carbon balance improved with Mn_2O_3 in the post-plasma compared with addition in the plasma. The increase in CO_2

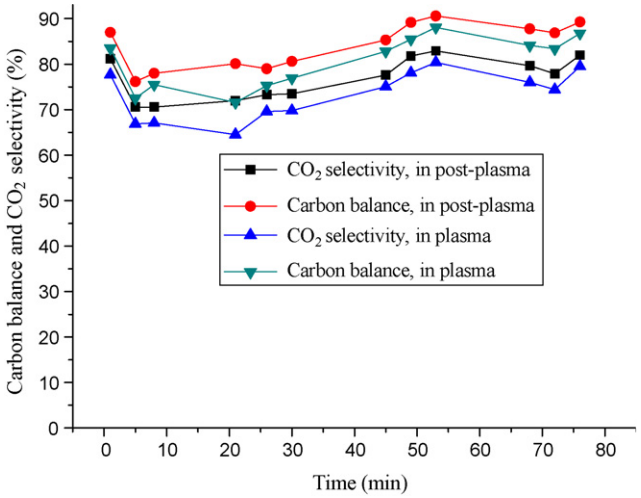

Fig. 4. CO_2 selectivity and carbon balance with the catalyst in plasma or in the post-plasma.

selectivity and carbon balance meant more toluene was oxidized into COx and less byproduct was produced.

Therefore, the combination of Mn_2O_3 in the post-plasma enhances toluene conversion and efficiently decreases O_3 concentration at the outlet. The CO_2 selectivity and carbon balance were also improved slightly. Catalysis in the post-plasma is superior to that in the plasma.

3.2. Influence factors

Study of the main factors in the post-plasma is helps to understand the performance of the removal of toluene and O_3, to investigate its mechanism, and to better to control the process.

3.2.1. Catalysts

It is shown in Table 1 that conversion of toluene via gas-feeding methods (b) by various catalysts follows the order: $CuO < Co_3O_4 < Mn_2O_3 < TiO_2 < Fe_2O_3$ and the corresponding conversion of O_3 follows the same order: $CuO < Co_3O_4 < Mn_2O_3 < TiO_2 < Fe_2O_3$. We can find that the conversion of toluene is positively correlated with that of O_3. O_3 conversion is also positively correlated to the catalyst BET surface area, except for Co_3O_4 and TiO_2. O_3 decomposition performance of metal oxides is closely related to their semiconductor type. The p-type semiconductor is better than the n-type [13]. TiO_2 showed good O_3 conversion in this study. Although TiO_2 is an nn-type semiconductor, it has the biggest surface area. Therefore, the adsorption capacity of catalysts also plays an important role in the conversion of toluene and O_3. The O_3 decomposition performance of different catalysts mainly depends on characteristics, such as the surface area and the semiconductor type. The results indicated that the performance of various catalysts for toluene conversion mainly depended on the performance for catalytic decomposition of O_3. It suggests that the performance for O_3 decomposition should be the focus in order to obtain highly reactive catalysts for VOCs such as toluene conversion in the post-plasma.

3.2.2. Humidity

Fig. 5 shows that toluene conversion is decreased with an increase in humidity in the gas flow. However, humidity has little influence on O_3 conversion. Toluene and O_3 conversion are greater in dry air. The decrease of toluene conversion can be partly ascribed to the decrease in O_3 conversion. Catalytic ozonation plays an important role in toluene oxidation. The water vapor prevented the adsorption of toluene on the catalyst because of competitive adsorption of H_2O [14]. What is more, water covered the surface of the catalyst [12] and poisoned the catalyst by occupying catalytic active centers [15–17]. Therefore, humidity should be controlled for optimum toluene and O_3 conversion.

The effect of humidity on toluene conversion in the system with catalysts in the post-plasma is similar to that in a system with catalysts in the plasma [18] and different from that in a plasma-only system. In the plasma-only system, an appropriate amount of water can enhance toluene conversion, and the optimal humidity

Table 1
Conversion of toluene and O_3 over various catalysts in the post-plasma (C_{ozone0} = 112 ppm)

Catalyst	Conversion of toluene (%)	Conversion of O_3 (%)	BET surface area (m^2/g)
Co_3O_4	33	71.5	12.3
CuO	44	83.9	6.4
Mn_2O_3	52	89.3	10.8
TiO_2	54	92.9	55.7
Fe_2O_3	64	94.6	14.6

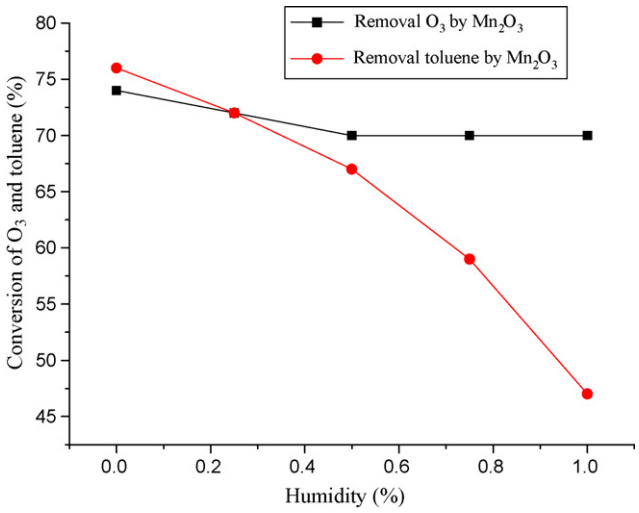

Fig. 5. Effect of humidity on toluene conversion and O_3 in the post-plasma.

3.2.3. Effect of O_3 concentration

O_3 concentration can be adjusted by the applied voltage and choice of carrier gas. With N_2 as carrier gas, no O_3 was formed, and there are only active species in the post-plasma. As shown in Fig. 6, little toluene can be removed in the post-plasma with N_2 as carrier. The result further directly demonstrated the insignificance of active species from the plasma and indirectly showed the importance of O_3 for the toluene conversion in the post-plasma. Conversion of toluene and O_3 both increase with an increase in the initial O_3 concentration. High O_3 concentration in the post-plasma favored the conversion of toluene. The oxidation of toluene was closely related to O_3 decomposition. The result also confirmed the importance of O_3 and catalytic ozonation in toluene removal. O_3 promoted toluene oxidation. The conversion of toluene is dependent on the O_3 catalytic decomposition.

3.3. Mechanism

Fig. 7 shows toluene conversion with Mn_2O_3 in the post-plasma and O_3-only reactor, respectively. The O_3-only reactor was connected to the post-plasma reactor through a buffer flask with capacity of 5 L. In the O_3-only reactor, active species from the

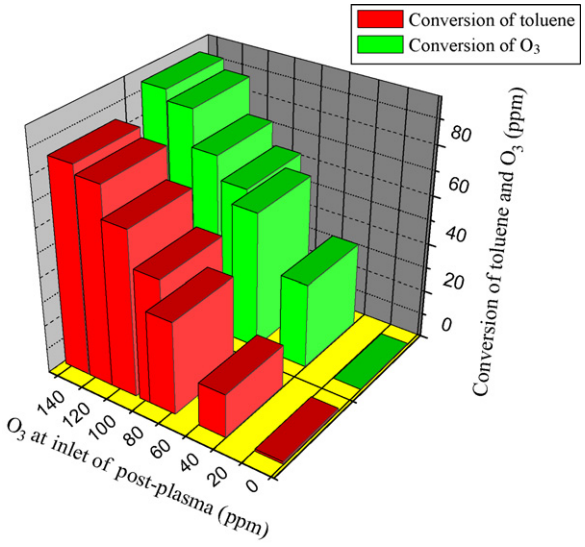

Fig. 6. Effect of O_3 concentration on toluene conversion and O_3 in the post-plasma.

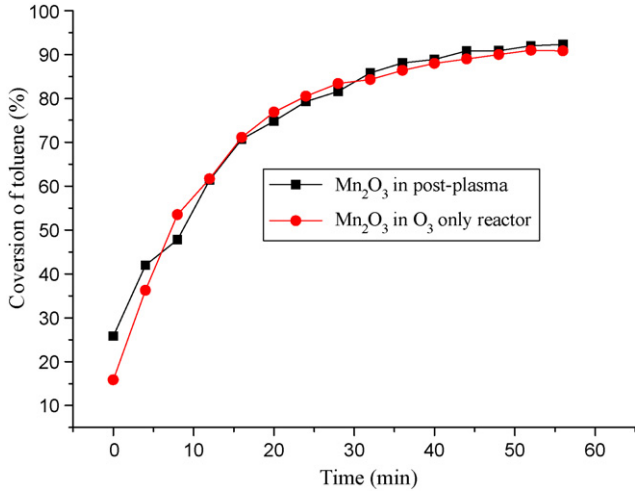

Fig. 7. Toluene conversion with Mn_2O_3 in the post-plasma and O_3-only reactor, respectively.

plasma were extinguished because of their microsecond lifetimes. It can be seen that Mn_2O_3 in the post-plasma has almost the same toluene conversion as that in the O_3-only reactor. The active species leaving the plasma are very short-lived [19,20]. There is no active species left except the long-lived O_3 in an O_3-only reactor. Therefore, O_3 is the most important oxidant in the post-plasma. The effect of active species discharged from the plasma can be neglected, as discussed above.

There has been little work on the kinetics and mechanism of the ozone decomposition reaction. A plausible mechanism for the Mn_2O_3 catalytic decomposition of O_3 and toluene was suggested in Fig. 8.

Toluene is adsorbed to the catalyst. O_3 is also adsorbed on a site of the catalyst to produce a free oxygen molecule and a surface oxygen atom and then the oxygen atom further oxidizes the toluene, which is activated by the catalyst, into H_2O and CO_2. Li et al. [21,22] and Dhandapani and Oyama [13] reported that O* was formed during O_3 decomposition. Futamura et al. [23] suggested that the active oxygen formed from the O_3 catalytic decomposition is should be $O(^3P)$. However, singlet oxygen, $O(^3P)$, has very short lifetime of about several tens nanoseconds in gas-phase, so it cannot stay longer. Therefore, the active oxygen formed from the O_3 catalytic decomposition cannot be singlet atomic oxygen. No assumptions were made about the nature of the active sites and the state of the adsorbed oxygen [13].

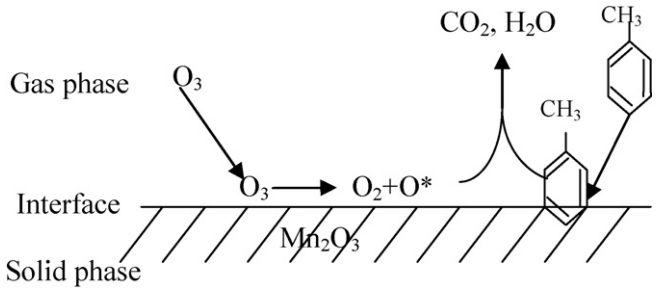

Fig. 8. Mechanism for Mn_2O_3 catalytic decomposition of O_3 and toluene.

3.4. Characterization of catalysts

Manganese oxide was mainly used in this study and was chosen for characterization. This was done with a thermo gravimetric analyzer (NETZSCH STA 409C, Germany), XRD (Rigaku, D/max-IIIA), SEM (1530 VP, LEO), and EDS (Inca 300, Oxford), respectively.

3.4.1. TG-DTA

Thermal analysis was performed in a Thermo gravimetric analyzer. The samples were heated in N_2 flowing at 30 ml/min, from 50 to 900 °C, at a rate of 10 °C/min.

The precursor of Mn_2O_3 is manganese nitrate. It can be observed in Fig. 9 that there is one sharp loss of weight and two smooth losses of weight. The sharp loss in mass of 41.96% was occurred between 180.7 and 210.5 °C, accompanied by a sharp exothermic peak. One of the smooth loss of weight occurred between 424.1 and 440.9 °C, and the other smooth loss of weight loss occurred between 513.7 and 551.3 °C, accompanied by two smooth endothermic peaks. The sharp loss of weight and sharp exothermic peak were mainly caused by the decomposition of the precursor, manganese nitrate. Manganese nitrate was decomposed into Mn_2O_3. The smooth loss of weight was mainly due to the crystallization of amorphous MnOx and crystal MnOx.

3.4.2. XRD

The X-ray diffraction (XRD) measurements were performed using an X-ray diffractometer with a scanning rate of 4°/min with the 2θ from 10° to 80°, using a monochromatized Cu Kα radiation (λ = 0.154 nm). The X-ray diffractometer was equipped with a heating device.

From the results of TG-DTA, when the manganese nitrate was calcined at the each temperatures of 200–600, the XRD pattern of

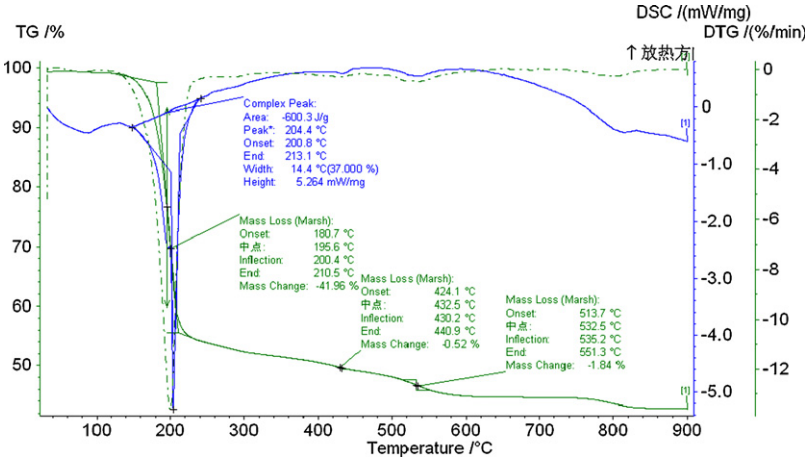

Fig. 9. TG-DTA plots for the dry $Mn(NO_3)_2$ at 10 °C/min heating rate in N_2.

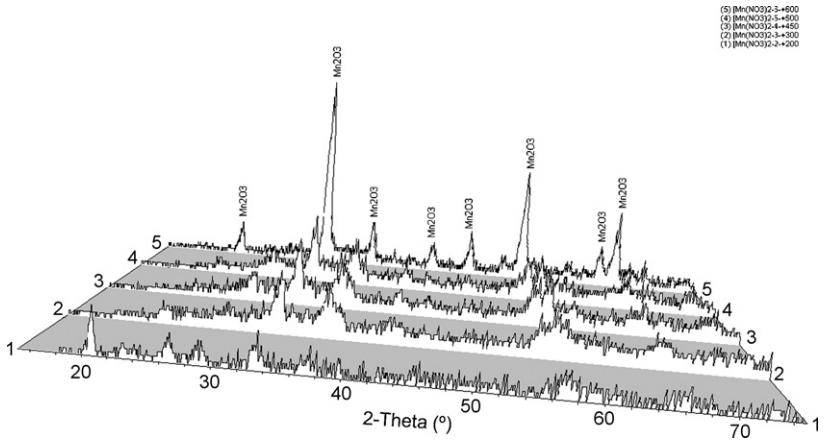

Fig. 10. XRD pattern of $Mn(NO_3)_2$ at different temperatures (1: 200 °C; 2: 300 °C; 3: 400 °C; 4: 500 °C; 5: 600 °C).

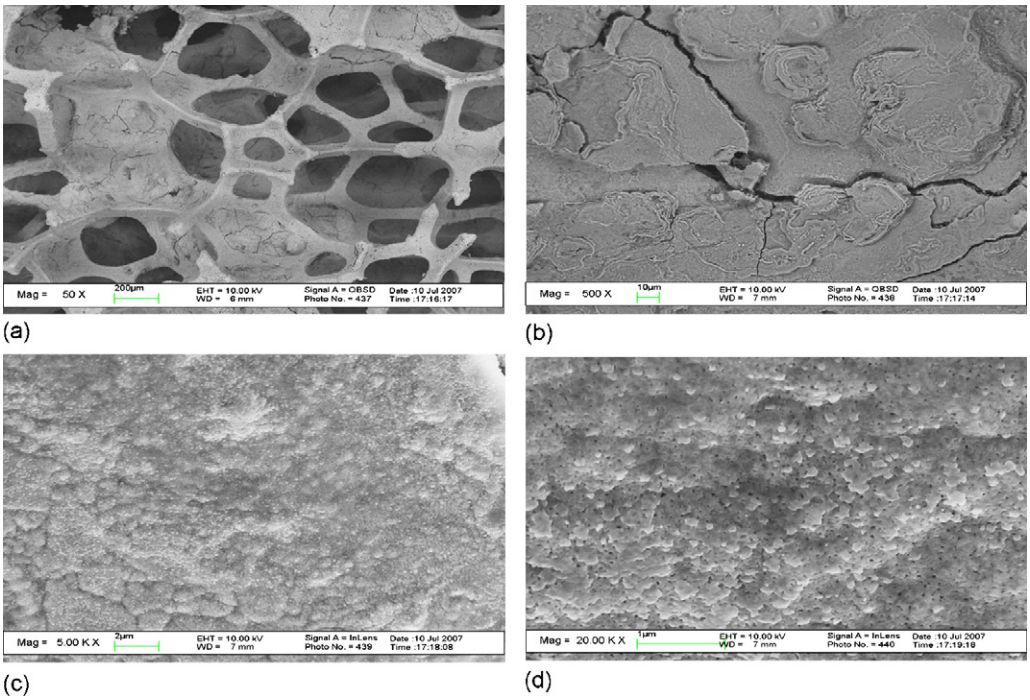

Fig. 11. SEM images of Mn_2O_3/nickel foam: (a) 50×, (b) 500×, (c) 5000 and (d) 20,000.

$Mn(NO_3)_2$ at each temperature shown in Fig. 10. Manganese nitrate was heated at the rate of 10/min. When the calcining temperature is lower than 400, MnOx showed ultra-fine or amorphous features of phase. When it was treated at 500, the diffraction peak of Mn_2O_3 appeared. Fine crystallites were ultimately obtained after the gel was treated at 600. All peaks are identified as Mn_2O_3. The optimal calcining temperature for Mn_2O_3 is about 600 °C.

3.4.3. SEM and EDS

Fig. 11 shows the SEM images of Mn_2O_3/nickel foam. SEM images of catalyst are amplified by 50, 500, 5,000 and 20,000 times, respectively. They indicate that Mn_2O_3 is loaded in disperse form on the surface of the nickel foam skeleton. Nickel foam is a special support. It is thin and porous, which enables the pressure drop in the reactor to be greatly reduced.

An EDS photograph of Mn_2O_3 is shown in Fig. 12. It can be seen that the surface of the catalyst was mainly covered with MnOx, i.e., Mn_2O_3. The Ni spectrum came from the nickel foam skeleton. Carbon was also found in the EDS photograph after the reaction. This demonstrates that carbonate was produced and deposited on

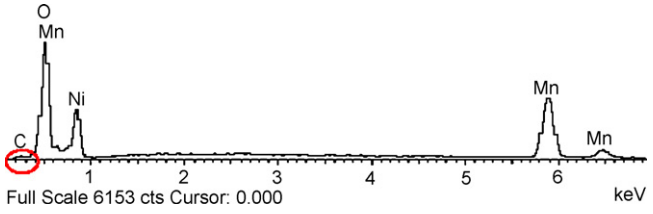

Fig. 12. EDS spectrum of Mn_2O_3 after reaction in the post-plasma.

the Mn_2O_3 during the reaction. The EDS result is in agreement with that of XRD.

4. Conclusions

The combination of catalysis in the post-plasma cannot only efficiently decrease the concentration of O_3 in the effluent but also greatly enhance the decomposition of toluene. The removal efficiency of toluene by different catalysts mainly depended on the performance of catalytic decomposition of O_3. O_3 can promote toluene oxidation, whereas water has a negative effect on toluene conversion. Catalytic ozonation was mainly responsible for toluene removal. The active oxygen from catalytic decomposition of O_3 further oxidizes the toluene.

Acknowledgment

The authors acknowledge the financial support of National Nature Science Foundation of China (20577011).

References

[1] S. Futamura, H. Einaga, H. Kabashima, L.Y. Hwan, Catalysis Today 89 (2004) 89.
[2] H. Huang, D. Ye, M. Fu, F. Feng, Plasma Chemistry and Plasma Processing 27 (2007) 577.
[3] T. Oda, Journal of Electrostatics 57 (2003) 293.
[4] S. Delagrange, L. Pinard, J.M. Tatibouet, Applied Catalysis B-Environmental 68 (2006) 92.
[5] Y.F. Guo, D.Q. Ye, K.F. Chen, J.C. He, Catalysis Today 126 (2007) 328.
[6] U. Roland, F. Holzer, F.D. Kopinke, Catalysis Today 73 (2002) 315.
[7] B.Y. Lee, S.H. Park, S.C. Lee, M. Kang, S.J. Choung, Catalysis Today 93 (2004) 769.
[8] H.H. Kim, S.M. Oh, A. Ogata, S. Futamura, Applied Catalysis B-Environmental 56 (2005) 213.
[9] F. Holzer, U. Roland, F.D. Kopinke, Applied Catalysis B-Environmental 38 (2002) 163.
[10] A. Ogata, H. Einaga, H. Kabashima, S. Futamura, S. Kushiyama, H.H. Kim, Applied Catalysis B-Environmental 46 (2003) 87.
[11] H.B. Huang, D.Q. Ye, B.C. Huang, M.L. Fu, Environmental Science & Technology (submitted for publication).
[12] Y.F. Guo, D.Q. Ye, K.F. Chen, Y.F. Tian, Plasma Chemistry and Plasma Processing 26 (2006) 237.
[13] B. Dhandapani, S.T. Oyama, Applied Catalysis B-Environmental 11 (1997) 129.
[14] P.Y. Zhang, F.Y. Liang, G. Yu, Q. Chen, W.P. Zhu, Journal of Photochemistry and Photobiology A-Chemistry 156 (2003) 189.
[15] H. Einaga, T. Ibusuki, S. Futamura, IEEE Transactions on Industry Applications 37 (2001) 1476.
[16] C.H. Cho, S.K. Ihm, Environmental Science & Technology 36 (2002) 1600.
[17] D.Q. Ye, H.B. Huang, W.L. Chen, R.H. Zeng, Plasma Science and Technology 10 (2008) 89.
[18] N. Yasyerli, G. Dogu, T. Dogu, B.J. McCoy, AIChE Journal 45 (1999) 291.
[19] I.S.N. Young Sun Mok, Chemical Engineering & Technology 22 (1999) 527.
[20] B. Eliasson, U. Kogelschatz, IEEE Transactions on Plasma Science 19 (1991) 309.
[21] W. Li, G.V. Gibbs, S.T. Oyama, Journal of the American Chemical Society 120 (1998) 9041.
[22] W. Li, S.T. Oyama, Journal of the American Chemical Society 120 (1998) 9047.
[23] S. Futamura, A.H. Zhang, H. Einaga, H. Kabashima, Catalysis Today 72 (2002) 259.